In-situ Microscopy Characterization of Cu(In,Ga)Se_2 Potential-Induced Degradation

Preprint

Chuanxiao Xiao, Chun-Sheng Jiang, Steven P. Harvey, Lorelle Mansfield, Christopher P. Muzzillo, Dana Sulas, Jun Liu, Steve Johnston, and Mowafak Al-Jassim

National Renewable Energy Laboratory

Presented at the 46th IEEE Photovoltaic Specialists Conference (PVSC 46)
Chicago, Illinois
June 16–21, 2019

NREL is a national laboratory of the U.S. Department of Energy
Office of Energy Efficiency & Renewable Energy
Operated by the Alliance for Sustainable Energy, LLC

This report is available at no cost from the National Renewable Energy Laboratory (NREL) at www.nrel.gov/publications.

Contract No. DE-AC36-08GO28308

Conference Paper
NREL/CP-5K00-73121
June 2019

In-situ Microscopy Characterization of Cu(In,Ga)Se_2 Potential-Induced Degradation

Preprint

Chuanxiao Xiao, Chun-Sheng Jiang, Steven P. Harvey, Lorelle Mansfield, Christopher P. Muzzillo, Dana Sulas, Jun Liu, Steve Johnston, and Mowafak Al-Jassim

National Renewable Energy Laboratory

Suggested Citation
Xiao, Chuanxiao, Chun-Sheng Jiang, Steven P. Harvey, Lorelle Mansfield, Christopher P. Muzzillo, Dana Sulas, Jun Liu, Steve Johnston, and Mowafak Al-Jassim. 2019. *In-situ Microscopy Characterization of Cu(In,Ga)Se_2 Potential-Induced Degradation: Preprint*. Golden, CO: National Renewable Energy Laboratory. NREL/CP-5K00-73121. https://www.nrel.gov/docs/fy19osti/73121.pdf.

NREL is a national laboratory of the U.S. Department of Energy
Office of Energy Efficiency & Renewable Energy
Operated by the Alliance for Sustainable Energy, LLC

This report is available at no cost from the National Renewable Energy Laboratory (NREL) at www.nrel.gov/publications.

Contract No. DE-AC36-08GO28308

Conference Paper
NREL/CP-5K00-73121
June 2019

National Renewable Energy Laboratory
15013 Denver West Parkway
Golden, CO 80401
303-275-3000 • www.nrel.gov

In-situ Microscopy Characterization of Cu(In,Ga)Se_2 Potential-Induced Degradation

Chuanxiao Xiao, Chun-Sheng Jiang, Steven P. Harvey, Lorelle Mansfield, Christopher P. Muzzillo, Dana Sulas, Jun Liu, Steve Johnston, and Mowafak Al-Jassim

National Renewable Energy Laboratory, Golden, CO 80401 USA

***Abstract* — We report on the role of sodium in potential-induced degradation (PID) of Cu(In, Ga)Se_2 (CIGS) solar cells. In-situ microscopy characterizations on AFM platform were performed on two stressed CIGS device under room temperature (RT) and high temperature (HT) at 85 °C. During PID stressing we observed depletion region gets wider as Na migrates, p-n junction becomes leaky at RT for over a month; and similar junction evolution was observed for HT-stressed sample, eventually the junction collapsed after 18 hours. The diode behaviors were confirmed by dark I-V measurement. Time-of-Flight secondary-ion mass spectrometry reveals that the Na accumulates on ZnO and CdS side, as well as the upper layer of CIGS layer. The results indicate that Na drifted by the voltage applied on the soda-lime glass, then diffuse through the whole device. And the sodium profiles have different points of evolution due to the temperature differences between the two stressed samples. The consistent results unambiguously show how Na from substrate glass causes PID in CIGS solar cells.**

***Index Terms* — CIGS, PID, in-situ microscopy, sodium, p-n junction.**

I. Introduction

Today it is increasingly important to investigate reliability in thin-film solar modules before their large penetration in the photovoltaic (PV) market. Cu(In,Ga)Se_2 (CIGS) solar cells have achieved a remarkable high efficiency of 22.9% in the recent development of incorporating alkali elements[1]–[4]. Sodium (Na) is known to improve the cell efficiency[3], [6], [7]; however, Na is also suspected to degrade the module performance via potential-induced degradation (PID)[8]–[11]. PID could cause devastating power reduction in PV modules[12], [13], so it is essential to understand the PID failure mechanism and address this problem.

In this paper, we extensively investigated the role of Na in a PID study of CIGS solar cells by Kelvin probe force microscopy (KPFM) and time-of-flight secondary-ion mass spectrometry (TOF-SIMS). Here, we applied *in-situ* KPFM characterization to study two CIGS devices that were stressed at room temperature (RT) and high temperature (HT) at 85°C. The CIGS solar cells have a soda-lime glass substrate, which is a major source of Na. The p-n junction was characterized during stressing. We observed junction evolution on both samples: the depletion width widens after a one-month RT stress, and the junction collapses after an 18-hour HT stress. Dark current-voltage (I-V) curves confirm the affected diode quality. TOF-SIMS revealed Na accumulation at ZnO and CdS layers for both samples, as well as the upper layer of CIGS. The 3-D results show similar trends, but at different points of evolution of the Na profiles due to the temperature differences between the stressed samples.

II. Experiment Details

The devices on soda-lime glass are a stack of Mo/CIGS/CdS/ZnO/ZnO:Al/metal grid; detailed architecture and parameters can be found in Ref. [14]. The device is manually cleaved with further ion milling to make a flat cross section for atomic force microscopy characterization[15].

The KPFM measures electrostatic potential on the sample surface in a 30-nm spatial resolution and a 10-mV potential resolution. *In-situ* KPFM monitors the potential evolution across the CIGS p-n junction on an AFM platform[16]. The experiment schematic is shown in Figure 1. A constant bias voltage of -1500 V was applied to the polished CIGS devices in short circuit. The backside of the glass substrate was grounded. The entire back was covered with silver paint to uniformly apply high voltage, and thus a homogenous degradation. One device was stressed at RT of ~25°C for more than one month; the other one was stressed at HT of ~85°C for 18 hours. Note that the cell is in short-circuit during the stressing.

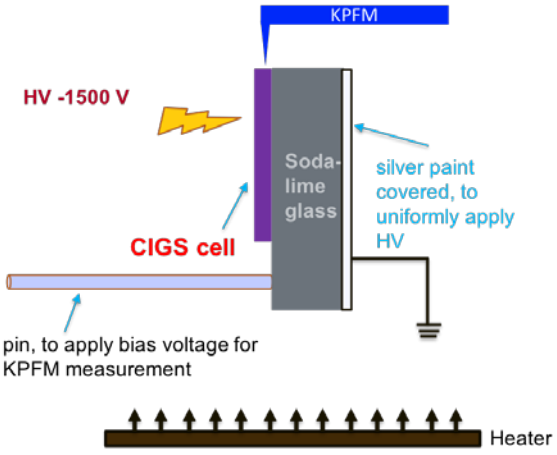

Fig. 1. Schematic of in-situ *PID stressing on AFM platform.*

After *in-situ* stressing, dark I-V curves were measured on the two stressed samples. We also used a sample without any PID stress but went through the whole ion-milling process. The unstressed sample served as a reference to ensure that there were no measurement artifacts. The Na distribution of RT-

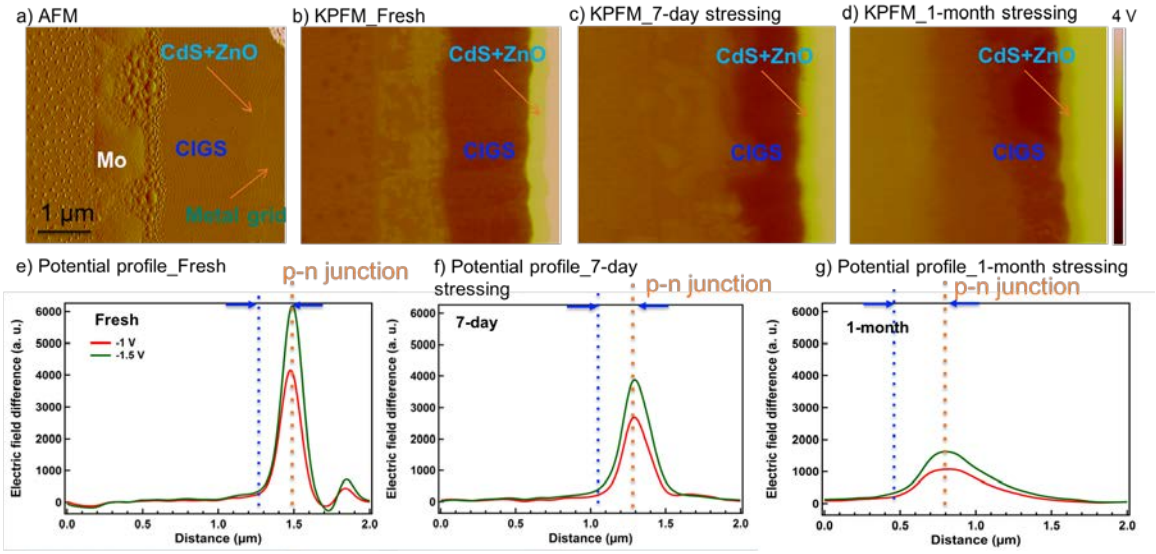

Fig. 2. KPFM results of RT-stressed CIGS cell.

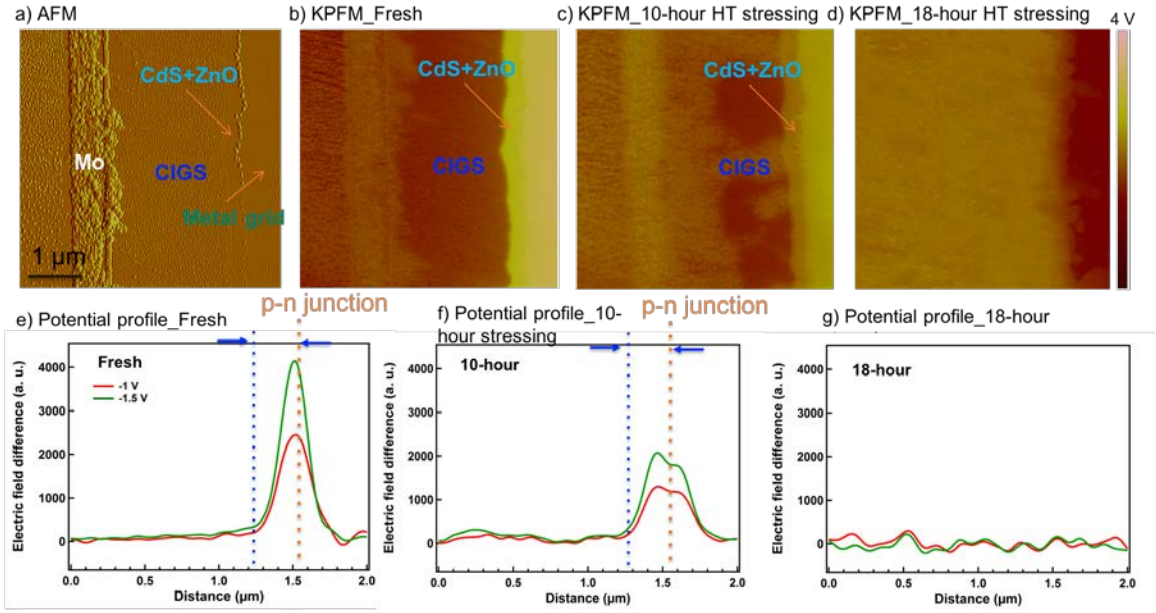

Fig. 3. KPFM results of HT-stressed CIGS cell.

stressed and HT-stressed samples was acquired by TOF-SIMS over a 100×100 μm^2 lateral area near the KPFM analyzed area, with a spatial resolution of 100 nm[17].

III. Results and Discussion

The high voltage difference between the two sides of soda-lime glass can effectively drive impurities such as Na to the device. Because the cell remains in short circuit during stressing, after Na drifts to the Mo layer the driving force for Na is diffusion, which follows Fick's laws of diffusion. Na is expected to affect the electrical properties of CIGS and CdS[18], and it further affects the p-n junction. To capture the dramatic change of electrical properties, we stressed two samples, one at RT and one at HT.

Figure 2 shows *in-situ* KPFM results of RT stressing, with data taken at the same location over a long period of more than one month. Figure 2a shows the AFM amplitude error image, which has a better contrast for different layers. Mo/CIGS/CdS+ZnO layers can be identified clearly. The data were acquired from an area with a metal grid to avoid probe-drop during scanning. We took the AFM and KPFM images under multiple bias voltages (Vbs) of 0 V, 1 V, and -1.5 V. Figure 2b shows the potential image of the fresh sample, 2c is

after 7-day PID stressing at -1.5 V, and 2d is after one-month stress at -1.5 V. The contrast of the potential images gets smaller during the PID stress.

We measure the bulk potential change under varying Vbs by measuring surface potential changes[19]. The Vb-induced change in the electric field was deduced by the first derivatives of the potential difference curves. Due to the limited space here, we only show the electric field curves. In Fig. 2e, the potential profiles of the fresh stage suggest a normal CIGS/CdS junction without degradation. The orange dashed line indicates the location of the p-n junction. The distance between the blue dashed line and the orange dashed line gives an estimation of a 200–300-nm depletion region width, consistent with CIGS doping of 2×10^{16} cm^{-3}. After PID stressing for 7 days, the electric-field peak intensity decreased significantly. The lower electric-field peak intensity suggests a weaker diode after PID stressing. The depletion width increased to ~400 nm, which suggests that the doping of CIGS or CdS gets smaller. Note that Na may not make the CIGS material higher p-doped, and a large amount of Na may act as an impurity or cause structural defects [20], which leads to more defective CIGS. The Na-induced defects may capture free carriers, which results in a larger depletion width (less effective p-doped) and a leaky junction. Furthermore, in CdS material Na can substitute in Cd sites, like the effect of Cu, which can cause deep-level defects in CdS (the valence band maximum [VBM] of CdS is ~0.5 eV lower than CIGS, so it is easier to create deep-level defects in CdS). After one-month stressing, the potential change under Vbs is smoother. To make a clear comparison, the scales of the potential profiles were intentionally made the same. After the long-term stressing, the diode becomes even weaker and the depletion width is further widened.

Similarly, we monitored the potential evolution along HT stressing at 85°C. The AFM amplitude error image in Fig. 3a distinguished different layers of the device. The KPFM image at the fresh stage taken at -1.5 V in Fig. 3b is similar to Fig. 2b. After 10 hours stressing, we mapped the potential image (Fig. 3c) at the same location. After 18 hours stressing, no significant potential change was observed around the CIGS/CdS interface, with results shown in Fig. 3d. The potential profiles are shown in Figs. 3e–g. The electric-field difference curve in Fig. 3e is measured at HT, and it is similar to the fresh cell results at RT. After 10 hours of HT stressing at -1500 V, the electric-field peak intensity dropped about half and the depletion width is similar. This suggests that a large amount of Na may quickly diffuse to the CIGS/CdS junction area and increase the leakage current. After 18 hours, the junction collapsed to a flat line. There is no electric field detectable around the p-n junction region, which indicates that the sample has a very weak equivalent shunt resistance and behaves as a resistor rather than a diode.

The KPFM results were confirmed by dark I-V measurements. Figure 4 shows the comparison of the three devices: fresh polished (black curve), RT-stressed for one month (red curve), and HT-stressed for 18 hours (green line). As a reference, we use the same sample preparation procedure to polish a device from the same piece. The stress-free fresh sample acts as a functional diode, with a small degree of edge shunting due to sample cutting and ion milling. The RT-stressed sample has a significantly increased reverse saturation current J_0, which indicates poor junction quality, and an increased diode ideality factor. The HT-stressed sample is a straight line, indicating complete junction failure. The I-V curves are consistent with the final stress stage of the KPFM results.

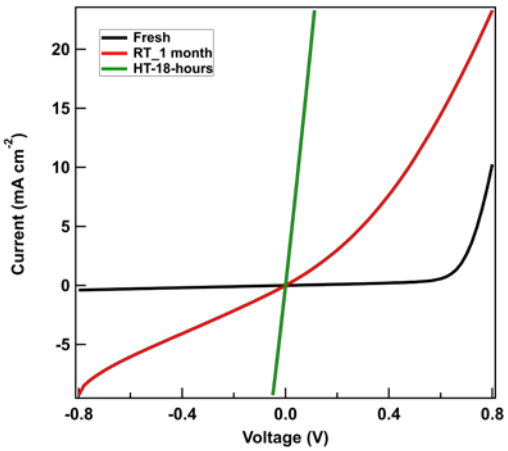

Fig. 4. Dark I-V curves of fresh polished, RT-stressed for one month, and HT-stressed for 18 hours samples.

To address the Na issue in detail, we performed TOF-SIMS measurements on the two stressed CIGS devices characterized by KPFM and dark I-V measurements; results are shown in Fig. 5. The samples were both rinsed with deionized water to remove surface sodium and the possibility of sputtering drive-in artifacts in TOF-SIMS analysis.

The 3-dimensional data show similar trends: both RT- and HT-stressed samples have Na accumulation at the transparent conductive oxide (TCO) and CdS layers and the CIGS near the CdS/CIGS interface (Figs. 5b, c). More Na is found on the Mo/glass region, indicating that Na+ ions drifted from the soda-lime glass. We observed different points of evolution of the Na profiles, most likely due to the temperature differences between the stressed samples. Figures 5d and 5e show the Na distribution in the upper CIGS layer. The RT-stressed sample seems to show Na mostly at grain boundaries in the CIGS and more uniformly incorporated at the TCO/CdS/CIGS region. The HT sample shows similar behavior, but a more laterally uniform Na distribution near the TCO/CdS/CIGS region. This is due to the different kinetics for the two experiments; the RT stressing lasts for more than one month, and if the high voltage were kept for a much longer time, then the Na should eventually shunt the device. These data suggest a PID degradation mechanism where the Na quickly diffuses through the CIGS grain boundaries and piles up at the TCO/CdS/CIGS region, at which point it also starts to diffuse into the CIGS grain interiors. Figure 5f shows a quantified Na profile over the

depth of the whole CIGS device. The Na concentration reaches 10^{20} cm^{-3} for the HT-stressed sample, and the CIGS upper layer has a concentration at 10^{19} cm^{-3}. This large amount of Na can effectively damage the p-n junction and cause a complete shunt for the device. For the RT-stressed sample, the Na peak is at a low 10^{19} cm^{-3} level, which can significantly alter the doping in both CIGS and CdS layers. The high contamination of Na in CdS makes it less n-doped, which causes the depletion to be wider, as observed in the KPFM potential profiles.

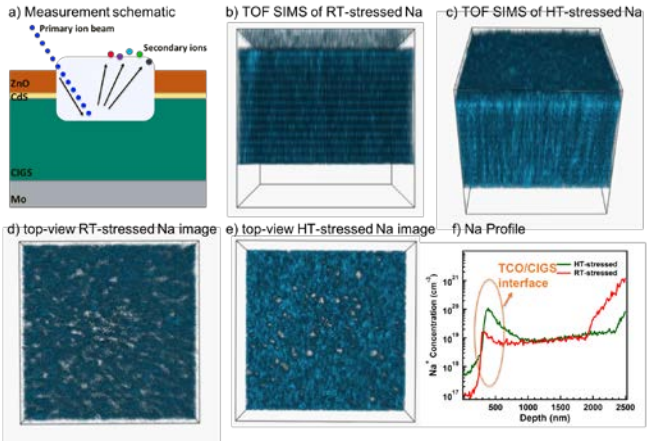

Fig. 5. TOF-SIMS results of RT- and HT-stressed samples.

IV. Conclusion

We revealed the role of Na in PID of CIGS solar cells with different temperature stressing. Two CIGS devices were stressed under RT and HT, respectively. The potential profiles were monitored by in-situ KPFM characterization, and we observed p-n junction evolution during PID stressing. The depletion region gets wider as Na starts to affect CIGS and CdS layers, while the junction becomes leaky. At HT, the Na diffusion is more serious and quickly shunts the whole device. Dark I-V curves confirm the degradation observed in KPFM profiles. TOF SIMS quantitatively determined the high concentration of Na at the TCO/CdS/CIGS interface. The consistent results revealed the role of Na in PID of CIGS solar cells.

References

[1] A. Chirilă *et al.*, "Potassium-induced surface modification of Cu(In,Ga)Se_2 thin films for high-efficiency solar cells," *Nat. Mater.*, vol. 12, no. 12, pp. 1107–1111, Dec. 2013.

[2] P. Jackson, R. Wuerz, D. Hariskos, E. Lotter, W. Witte, and M. Powalla, "Effects of heavy alkali elements in Cu(In,Ga)Se2 solar cells with efficiencies up to 22.6%," *Phys. Status Solidi RRL – Rapid Res. Lett.*, vol. 10, no. 8, pp. 583–586.

[3] J. M. Raguse, C. P. Muzzillo, J. R. Sites, and L. Mansfield, "Effects of Sodium and Potassium on the Photovoltaic Performance of CIGS Solar Cells," *IEEE J. Photovolt.*, vol. 7, no. 1, pp. 303–306, Jan. 2017.

[4] Y. Sun *et al.*, "Review on Alkali Element Doping in Cu(In,Ga)Se2 Thin Films and Solar Cells," *Engineering*, vol. 3, no. 4, pp. 452–459, Aug. 2017.

[5] "Potassium-induced surface modification of Cu(In,Ga)Se2 thin films for high-efficiency solar cells | Nature Materials." [Online]. Available: https://www.nature.com/articles/nmat3789. [Accessed: 26-May-2018].

[6] C.-S. Jiang *et al.*, "Local built-in potential on grain boundary of Cu(In,Ga)Se2 thin films," *Appl. Phys. Lett.*, vol. 84, no. 18, pp. 3477–3479, Apr. 2004.

[7] D. Colombara *et al.*, "Sodium enhances indium-gallium interdiffusion in copper indium gallium diselenide photovoltaic absorbers," *Nat. Commun.*, vol. 9, no. 1, p. 826, Feb. 2018.

[8] V. Fjällström *et al.*, "Potential-Induced Degradation of CuIn$_1-x hboxGa_x$ Se_2 Thin Film Solar Cells," *IEEE J. Photovolt.*, vol. 3, no. 3, pp. 1090–1094, Jul. 2013.

[9] S. Yamaguchi *et al.*, "Potential-induced degradation of Cu(In,Ga)Se2 photovoltaic modules," *Jpn. J. Appl. Phys.*, vol. 54, no. 8S1, p. 08KC13, Jul. 2015.

[10] V. Fjällström *et al.*, "Recovery After Potential-Induced Degradation of CuIn$_bf 1-bm x$ $Ga_{bm\ x}Se_{bf\ 2}$ Solar Cells With CdS and Zn(O,S) Buffer Layers," *IEEE J. Photovolt.*, vol. 5, no. 2, pp. 664–669, Mar. 2015.

[11] S. Boulhidja, A. Mellit, and S. Voswinckel, "Potential-induced degradation test on CIGS photovoltaic modules," in *2017 5th International Conference on Electrical Engineering - Boumerdes (ICEE-B)*, 2017, pp. 1–4.

[12] E. Schneller, N. S. Shiradkar, and N. G. Dhere, "Performance variation of commercially available modules after six months of outdoor system voltage stress testing," in *2014 IEEE 40th Photovoltaic Specialist Conference (PVSC)*, 2014, pp. 3216–3219.

[13] J. Berghold *et al.*, "PID: from material properties to outdoor performance and quality control counter measures," in *Reliability of Photovoltaic Cells, Modules, Components, and Systems VIII*, 2015, vol. 9563, p. 95630A.

[14] I. Repins *et al.*, "19·9%-efficient ZnO/CdS/CuInGaSe2 solar cell with 81·2% fill factor," *Prog. Photovolt. Res. Appl.*, vol. 16, no. 3, pp. 235–239.

[15] C. Xiao *et al.*, "Locating the electrical junctions in Cu(In,Ga)Se2 and Cu2ZnSnSe4 solar cells by scanning capacitance spectroscopy," *Prog. Photovolt. Res. Appl.*, vol. 25, no. 1, pp. 33–40, Jan. 2017.

[16] C. Xiao *et al.*, "Development of in-situ high-voltage and high-temperature stressing capability on atomic force microscopy platform," *Sol. Energy*, vol. 158, pp. 746–752, Dec. 2017.

[17] S. P. Harvey *et al.*, "Investigating PID shunting in polycrystalline silicon modules via multiscale, multitechnique characterization," *Prog. Photovolt. Res. Appl.*, vol. 26, no. 6, pp. 377–384.

[18] C. P. Muzzillo *et al.*, "Potential-Induced Degradation of Cu(In,Ga)Se2Solar Cells: Alkali Metal Drift and Diffusion Effects," *IEEE J. Photovolt.*, vol. 8, no. 5, pp. 1337–1342, Sep. 2018.

[19] C. Xiao *et al.*, "Junction Quality of SnO2-Based Perovskite Solar Cells Investigated by Nanometer-Scale Electrical Potential Profiling," *ACS Appl. Mater. Interfaces*, vol. 9, no. 44, pp. 38373–38380, Nov. 2017.

[20] S.-H. Wei, S. B. Zhang, and A. Zunger, "Effects of Na on the electrical and structural properties of CuInSe2," *J. Appl. Phys.*, vol. 85, no. 10, pp. 7214–7218, May 1999.